A numerical method to determine interdiffusion coefficients of Cu6Sn5 and Cu3Sn intermetallic compounds

Article *in* Intermetallics · September 2013

DOI: 10.1016/j.intermet.2013.04.005

CITATIONS
14

READS
233

3 authors:

Jianfeng Li
University of Nottingham
115 PUBLICATIONS **2,013** CITATIONS

SEE PROFILE

Pearl Agyakwa
University of Nottingham
45 PUBLICATIONS **783** CITATIONS

SEE PROFILE

Mark Johnson
University of Nottingham
304 PUBLICATIONS **3,702** CITATIONS

SEE PROFILE

Intermetallics 40 (2013) 50–59

Contents lists available at SciVerse ScienceDirect

Intermetallics

journal homepage: www.elsevier.com/locate/intermet

A numerical method to determine interdiffusion coefficients of Cu_6Sn_5 and Cu_3Sn intermetallic compounds

J.F. Li*, P.A. Agyakwa, C.M. Johnson

Department of Electrical and Electronic Engineering, The University of Nottingham, University Park, Nottingham NG7 2RD, United Kingdom

ARTICLE INFO

Article history:
Received 25 January 2013
Received in revised form
13 March 2013
Accepted 9 April 2013
Available online 7 May 2013

Keywords:
A. Intermetallics, miscellaneous
B. Diffusion
C. Joining
D. Phase interfaces
E. Simulations, atomistic

ABSTRACT

A fixed-grid source-based numerical method has been developed to simulate the diffusion-controlled growth of Cu_6Sn_5 and Cu_3Sn intermetallic compounds (IMCs) and other many layers of IMCs. Data fittings of measured thicknesses of the IMCs to the simulated results can be further employed to determine the interdiffusion coefficients for the IMCs. Compared with the existing analytical methods, the present numerical method is not only more accurate, but also applicable to a wider range of experimental results. We report here the detailed formulation of the relevant equations, and compare and validate the present numerical method using experimental thicknesses of Cu_6Sn_5 and Cu_3Sn IMCs from both the existing literature and the experiment of our own. The results obtained provide new insight into the interdiffusion coefficients for the Cu_6Sn_5 and Cu_3Sn IMCs formed between Cu and Sn or Sn-based solders, or other many layers of IMCs formed in similar metal/metal systems.

1. Introduction

It is important to understand growth kinetics of intermetallic compounds (IMCS) formed during metallic interfacial reactions for studying reliability in a wide range of applications. For example, the formation of some Cu_6Sn_5 and Cu_3Sn IMCs during soldering is necessary to achieve good adhesion between Sn-based solders and Cu when Cu is used as contact metallizations on semiconductor devices and/or supporting substrates in electronic packaging [1–3]. However, excessive growth of the IMCs during extended soldering and/or service may result in brittle fracture of the joints [1,3]. Therefore, there has been a continuous effort in modelling and simulation to understand the growth kinetics of the Cu_6Sn_5 and Cu_3Sn IMCs in Sn-based solders/Cu systems [1–10].

During the soldering of a Sn-based solder, the formation and growth of Cu_6Sn_5 and Cu_3Sn IMCs is quite complicated and may involve multiple simultaneous processes [11–14]. The latter may include the dissolution of Cu atoms from the Cu substrate and/or the formed Cu_6Sn_5 IMC into the liquid Sn-based solder; the reaction between Cu atoms and Sn atoms, and the precipitation/nucleation of Cu–Sn IMCs on the top of Cu substrate; the solidification of Cu–Sn IMCs from supersaturated liquid solder; and lattice and/or grain boundary diffusion of Cu and Sn atoms in the formed Cu–Sn IMCs. In addition, grain boundary grooving, grain coarsening, grain faceting and grain coalescing also influence the growth kinetics of the IMCs [15]. Therefore, only in a few studies [5–7], have attempts been made to model the growth kinetics of Cu_6Sn_5 IMC in the liquid/solid interfacial reaction by a ripening process in which the driving force is the Gibbs–Thomson effect and/or grain boundary/molten channel controlled growth.

In a wealth of studies on the solid interfacial reaction between Sn-based solders and various types of Cu contact metallizations, the growth kinetics of both Cu_6Sn_5 and Cu_3Sn IMCs were explained in terms of diffusion-controlled growth, but described with the parabolic growth law only [1,2,8,9]. This is because in these studies, the solders were first soldered onto the Cu substrates through liquid/solid interfacial reaction during the reflowing processes, resulting in the formation of some Cu_6Sn_5 and probably plus Cu_3Sn IMCs through quite complicated processes as aforementioned. Then the soldered samples were placed into specific thermal storage to observe the thickening of the Cu_6Sn_5 and Cu_3Sn IMCs with ageing time. However, the existing analytical methods for diffusion-controlled growth kinetics, such as the Heumann method [16] and Wagner's method [4,10,17], have been developed and applied to diffusion couples where the initial thicknesses of the IMCs were zero.

* Corresponding author. Department of Electrical and Electronic Engineering, The University of Nottingham, Room 511, Tower Building, University Park, Nottingham NG7 2RD, United Kingdom. Tel.: +44 115 846 6890; fax: +44 115 951 5616.
E-mail addresses: Jianfeng.Li@nottingham.ac.uk, ljfwxy@yahoo.com (J.F. Li).

0966-9795
http://dx.doi.org/10.1016/j.intermet.2013.04.005

Nomenclature

$a's$	coefficients in the numerical scheme
b	parameter related to "Molar fraction per Molar volume" at previous time step, and the "latent Molar fraction per Molar volume of phase change at present time step in numerical scheme
D	interdiffusion coefficient [m^2 s^{-1}]
Δd	a small "sensible Molar fraction per Molar volume used in numerical scheme [mol m^{-3}]
N	Molar fraction
N_{Sn}	Molar fraction of Sn
N_V	"sensible Molar fraction per Molar volume" [mol m^{-3}]
ΔN_V	"latent Molar fraction per Molar volume of phase change" [mol m^{-3}]
$S(t)$	position of moving phase interface at time t [m]
t	time [s]
V	molar volume [m^3 mol^{-1}]
x	position coordinate [m]

Superscript

0	old value at previous time step
+	Right boundary of a phase, or right side of a moving interface
−	Left boundary of a phase, or left side of a moving interface

Subscript

i	phase i
Int	Integrated
E, *e*	east neighbouring node
P	node point
W, *w*	west neighbouring node

In the existing literature [3,10,16], the interdiffusion coefficients or integrated interdiffusion coefficients for the Cu_6Sn_5 and Cu_3Sn IMCs were obtained using the Heumann method and Wagner's method from the experimental results of Cu/Sn, Cu/Cu_6Sn_5 and Cu_3Sn/Sn diffusion couples. In the existing literature [18], the interdiffusion coefficients for Cu_6Sn_5 and Cu_3Sn IMCs were re-calculated using a combined analytical and numerical method from the same experimental results of the Cu/Sn diffusion couples reported in Ref. [16].

The present work is concerned with a numerical model to simulate the diffusion-controlled simultaneous growth of two adjacent Cu_6Sn_5 and Cu_3Sn IMCs in the Sn-based solder/Cu system. In combination with data fittings, this numerical method can be used to determine the interdiffusion coefficients for the Cu_6Sn_5 and Cu_3Sn IMCs formed in the samples with arbitrary initial thicknesses of the different phases. The developed numerical method is evaluated against the interdiffusion coefficients or integrated interdiffusion coefficients reported in Refs. [10,16,18]. In particular, systematic errors existing in the reported data are pointed out and discussed.

This paper starts with the mathematical formulation and schemes used in numerical procedures for the numerical method. Then the developed numerical method is compared and evaluated using the results of the Cu/Sn, Cu/Cu_6Sn_5 and Cu_3Sn/Sn diffusion couples reported in Refs. [10,16,18]. Following this, the numerical method is applied to calculate the thicknesses and extract the integrated interdiffusion coefficients for the Cu_6Sn_5 and Cu_3Sn layers formed in one Sn-3.8Ag-0.7Cu/Cu system. Although the principal motivation for this work is to develop a numerical method to determine more accurately and provide insight into the interdiffusion coefficients of the Cu_6Sn_5 and Cu_3Sn IMCs in the Sn-based solder/Cu system, the methodology and understanding developed in this work is expected to be applicable to other many layers of IMCs formed during similar metallic interfacial reactions.

2. Numerical method

2.1. Mathematical description of the problem

The present modelling to calculate the thicknesses of the Cu_6Sn_5 and Cu_3Sn layers is an extension of a previously developed fixed-grid numerical modelling of transient liquid phase bonding and other diffusion controlled phase changes [19]. It is still considers one-dimensional diffusion-controlled phase change and moving interface problems. However, it extends from two phases to four phases, with emphasis on the growth of two adjacent IMCs with a narrow homogeneity range, and uses the growth of Cu_6Sn_5 and Cu_3Sn layers in the Sn-based solder/Cu systems as one example, see Fig. 1. In such one-dimensional diffusion-controlled growth of two adjacent IMC layers, the effects of the IMCs nucleation, non-equilibrium defects and short-circuit paths such as dislocations, grain boundaries and external surfaces are all ignored. It is more applicable to the solid solder/Cu reactive diffusion. In order for the change of Molar volume of the solute in the different phases to be further taken into account, the governing equations based on Fick's diffusion law are given by:

$$\frac{\partial[N_{Sn}(x,t)/V(x,t)]}{\partial t}=\frac{\partial}{\partial x}\left[D_i\frac{\partial[N_{Sn}(x,t)/V(x,t)]}{\partial x}\right], \quad S_{i-1}(t)\langle x<S_i(t), \quad i=1,\ldots,4 \tag{1}$$

$$D_i\frac{\partial[N_{Sn}(x,t)/V(x,t)]}{\partial x}\bigg|_{x=S_i(t)^-}-D_{i+1}\frac{\partial[N_{Sn}(x,t)/V(x,t)]}{\partial x}\bigg|_{x=S_i(t)^+} =\left[N_i^+/V_i^+-N_{i+1}^-/V_{i+1}^-\right]\frac{\partial S_i(t)}{\partial t}, \quad x=S_i(t) \quad i=1,\ldots,3 \tag{2}$$

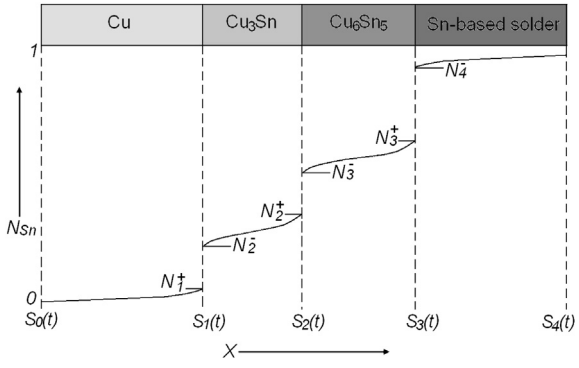

Fig. 1. Schematic illustration of the profile of Molar fraction N_{Sn} across a Cu/Sn-based solder joint at the instant time of t.

They are subject to the following boundary conditions:

$$\frac{\partial[N_{Sn}(x,t)/V(x,t)]}{\partial x} = 0 \quad x = S_0(0) \tag{3a}$$

$$\frac{\partial[N_{Sn}(x,t)/V(x,t)]}{\partial x} = 0 \quad x = S_4(0) \tag{3b}$$

And the initial conditions can be given as:

$$N_{Sn}(x,t)/V(x,t) = N_i(x,0)/V_i(x,0) \quad S_0(0) \le x \le S_4(0) \tag{4}$$

A numerical approach is generally required to solve the above equations. In principle, both variable and fixed-grid discretisation methods can be used. However, it is not convenient to use the variable grid discretisation method which has to track three moving phase-change interfaces, across which step changes in Molar fraction must be satisfied and whose locations are unknown *a-priori*. Therefore, the fixed-grid method will be employed in the present work. Following our previous work reported in Ref. [19], we may define a so-called "sensible Molar fraction per unit Molar volume" as:

$$N_{VSn}(x,t) = N_{Sn}(x,t)/V(x,t) - \Delta N_V \tag{5}$$

and a "latent Molar fraction per unit Molar volume of phase change" as:

$$\Delta N_V = \Delta N_{V1} + \Delta N_{V2} + \Delta N_{V3} \tag{6}$$

where

$$\Delta N_{Vi} = \begin{cases} N_{i+1}^-/V_{i+1}^- - N_i^+/V_i^+ - \Delta d_i, & N_{Sn}(x,t) \ge N_{i+1}^-,\ i = 1,\ldots,3 \\ 0 & N_{Sn}(x,t) \le N_i^+ \end{cases} \tag{7}$$

Then Eqs. (1) and (2) can be transformed into a unique equation for the four phases and three moving interfaces:

$$\frac{\partial N_{VSn}(x,t)}{\partial t} = \frac{\partial}{\partial x}\left(D(x,t)\frac{\partial N_{VSn}(x,t)}{\partial x}\right) - \frac{\partial \Delta N_V}{\partial t}, \quad S_0(0) < x < S_4(0) \tag{8}$$

with the boundary conditions:

$$\frac{\partial N_{VSn}(x,t)}{\partial x} = 0 \quad x = S_0(0) \tag{9a}$$

$$\frac{\partial N_{VSn}(x,t)}{\partial x} = 0 \quad x = S_4(0) \tag{9b}$$

and the initial conditions:

$$N_{VSn}(x,t) = N_i(x,0)/V_i(x,0) - \Delta N_V, \quad S_0(0) \le x \le S_4(0) \tag{10}$$

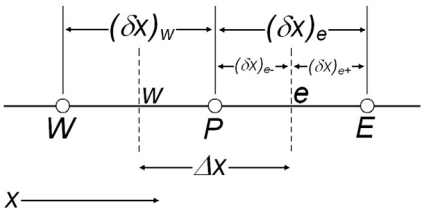

Fig. 2. Grid-point cluster and the relevant geometric parameters.

Equation (8) is essentially the same as the energy equation that takes account of heat conduction only for describing the phase change of melting and solidification and expressed in terms of sensible enthalpy. Here, the "Molar fraction per unit Molar volume", "latent Molar fraction per unit Molar volume of phase change" and diffusion coefficient are used to replace the sensible enthalpy, latent heat of fusion and thermal diffusivity in the energy equation. However, it should be pointed out that the present Eq. (8) includes more phases and more moving interfaces than those in the energy equation for describing the phase change of melting and solidification. Eqs. (5)–(10) formulate the mathematical description of the current model for diffusion-controlled growth of Cu_6Sn_5 and Cu_3Sn layers in the Sn-based solder/Cu systems and other similar diffusion-controlled phase change process. They are the main contribution of the present work and are readily solved using the fixed-grid source-based method [20,21].

2.2. Numerical procedures

The numerical procedures are similar to those in our previous work [19]. The coordinate x in Fig. 1 is first discretised into a fixed grid consisting of M nodes. Then the governing equations and boundary conditions formulated in Eqs. (5)–(10) are solved using the volume-controlled finite-difference method outlined by Patankar [22]. Referring to Fig. 2, the governing equation, Eq. (5), is discretized using the fully implicit discretisation scheme:

$$a_P N_P = a_E N_E + a_W N_W + b \tag{11}$$

where the subscripts, P, E and W, indicate the appropriate nodal values, the 'a' terms are coefficients dependent on the fluxes of the "sensible Molar fraction per unit Molar volume" and the "latent Molar fraction per unit Molar volume of phase change" into the Pth control volume, and the parameter, b, includes the terms associated with the evaluation of "sensible Molar fraction per unit Molar volume" at the previous time step, and the "latent Molar fraction per unit Molar volume of phase change". The terms related to the "latent Molar fraction per unit Molar volume of phase change" are discretized according to the following expression:

$$\frac{\partial \Delta N_V}{\partial t} = \frac{\Delta N_V(N_{VSn,P}) - \Delta N_V\left(N_{VSn,P}^0\right)}{\Delta t} = \begin{cases} 0, & N_{VSn,P}^0 \le V_{VSn,1}^+, \quad N_{VSn,P} \le V_{VSn,1}^+ \quad \text{or} \quad N_{VSn,P}^0 \ge V_{VSn,4}^-, \quad N_{VSn,P} \ge V_{VSn,4}^- \\ \dfrac{k(N_{VSn,P})}{\Delta t} N_{VSnP} - \left[\dfrac{k(N_{VSn,P})}{\Delta t} N_{VSn}^{Tem} + \dfrac{\Delta N_V\left(N_{VSn,P}^0\right)}{\Delta t}\right], & Otherwise \end{cases} \tag{12}$$

where the superscript, 0, indicates the nodal value at the previous time step, and:

$$\Delta N_V\left(N_{VSn,P}\right) = \sum_{i=1}^{3} \Delta N_i \min\left[\max\left(0, \frac{N_{VSn,P} - N^{+}_{VSn,i}}{\Delta d_i}\right), 1\right] \quad (13)$$

$$D_P = \left[\frac{f_i}{D_{i+1}} + \frac{1-f_i}{D_i}\right]^{-1} \quad (18)$$

$$k\left(N_{VSn,P}\right) = \frac{\sum_{i=1}^{3}\left(N^{-}_{i+1}/V^{-}_{i+1} - N^{+}_{i}/V^{+}_{i}\right)\ \max\left[0, \dfrac{N_{VSn,P} - N^{+}_{VSn,i}}{abs\left(N_{VSn,P} - N^{+}_{VSn,i}\right)}\right]}{\max\left\{\left(N_{VSn,P} - N^{Tem}_{VSn}\right),\ \sum_{i=1}^{3}\Delta d_i \max\left[0, \dfrac{N_{VSn,P} - N^{+}_{VSn,i}}{abs\left(N_{VSn,P} - N^{+}_{VSn,i}\right)}\right]\right\}} \quad (14)$$

$$N^{Tem}_{VSn} = \begin{cases} N^{+}_{VSn,1}, & N_{VSn,P} > N^{+}_{VSn,1},\ N_{VSn,P} \le N^{+}_{VSn,2} \\ N^{+}_{VSn,2} - \Delta d_1, & N_{VSn,P} > N^{+}_{VSn,2},\ N_{VSn,P} \le N^{+}_{VSn,3} \\ N^{+}_{VSn,3} - \Delta d_1 - \Delta d_2, & N_{VSn,P} > N^{+}_{VSn,3} \end{cases} \quad (15)$$

$$\Delta d_i = \frac{N^{-}_{i+1}/V^{-}_{i+1} - N^{+}_{i}/V^{+}_{i}}{N^{-}_{2}/V^{-}_{2} - N^{+}_{1}/V^{+}_{1}}\Delta d, \quad i = 1,2,3 \quad (16)$$

where a small "sensible Molar fraction per unit Molar volume" interval, e.g., $\Delta d = 1.0 \times 10^{-7}$ to 1.0×10^{-10} Molar/μm^3 depending on a particular simulation case, is employed to describe the diffusion-controlled phase change. Such a Δd is similar to a small temperature interval used to describe the phase change of melting and solidification [20].

During numerical iteration, Eqs. (13) and (14) are updated according to the nodal "sensible Molar fraction per unit Molar volume" obtained at the previous iteration step. This numerical scheme is somewhat different from that used in the standard fixed-grid source-based method, where the latent heat of fusion is directly updated using an appropriate formulation of the latent heat function [20,21]. In the present case, the "latent Molar fraction per unit Molar volume of phase change" has been linearised using Eq. (14), which was found to speed up the convergence of the iteration significantly.

With Eq. (12) and referring to Fig. 2, the '*a*' coefficients and the '*b*' parameter in Eq. (11) are given by:

$$a_E = \frac{D_e}{(\delta x)_e} \quad (17a)$$

$$a_W = \frac{D_w}{(\delta x)_w} \quad (17b)$$

$$b = \frac{\Delta x}{\Delta t}\left[k\left(N_{VSn,P}\right)N^{Tem}_{VSn} + \Delta N_V\left(N^{0}_{VSn,P}\right) + N^{0}_{VSn,P}\right] \quad (17c)$$

$$a_P = a_E + a_W + \frac{\Delta x}{\Delta t}\left[1 + k\left(N_{VSn,P}\right)\right] \quad (17d)$$

where the diffusion coefficients, D_e and D_w at the boundaries of a control volume should be the harmonic mean, rather than the arithmetic mean, as described in detail in Ref.[22]. Also, it is important to take a similar approach for updating the diffusion coefficient for any node whose "sensible Molar fraction per unit Molar volume" is between $N^{+}_{VSn,i}$ and $N^{-}_{VSn,i+1}$:

where

$$f_i = \frac{N_{VSn,P} - N^{+}_{VSn,i}}{\Delta d_i} \quad (19)$$

Otherwise, the simulation result may be physically unrealistic. For each step of the iteration procedure, the group of discretised equations for all the nodes is solved using the standard TriDiagonal-Matrix Algorithm [22]. Within each time step, calculation convergence was verified after the absolute residues of all the "sensible Molar fraction per unit Molar volume" values were three orders of magnitude lower than the selected small "sensible Molar fraction per unit Molar volume" interval, Δd. Once the converged "sensible Molar fraction per unit Molar volume" values are obtained, the moving interface between two phases is calculated using the following reverse function:

$$s^{+}_{i}(t) = x\Big|_{N_{VSn}(x,t)=N^{+}_{VSn,i}} = N^{-1}_{VSn}(N^{+}_{VSn,i}, t) \quad (20)$$

In addition, another moving interface expressed as:

$$s^{-}_{i+1}(t) = x\Big|_{N_{VSn}(x,t)=N^{-}_{VSn,i+1}} = N^{-1}_{VSn}(N^{-}_{VSn,i+1}, t) \quad (21)$$

is also calculated and compared with the interface $s^{+}_{i}(t)$. In the present work, they are both determined using linear interpolation of the nodal "sensible Molar fraction per unit Molar volume" values. Unless the average "sensible Molar fraction per unit Molar volume" of a material system is between $N^{+}_{VSn,i}$ and $N^{-}_{VSn,i+1}$, $s^{+}_{i}(t)$ and $s^{-}_{i+1}(t)$ should be very close to each other. Otherwise, as demonstrated in a pervious paper [19], a reduced small "sensible Molar fraction per unit Molar volume" interval, Δd, or an increased number of nodes, should be employed for achieving solutions which reasonably reflect the jump condition at all moving interfaces. However, this generally requires more computation effort. In the present work, the values of Δd and the numbers of nodes chosen in all simulation cases have been taken to ensure that the difference between $s^{+}_{i}(t)$ and $s^{-}_{i+1}(t)$ was less than 0.005 μm.

Once all the moving interfaces are calculated, it is straightforward to obtain the thicknesses of the different phases with respect to time.

2.3. Data fittings to determine interdiffusion coefficients

Data fittings of measured thicknesses of Cu_6Sn_5 and Cu_3Sn IMC layers to those simulated using the above numerical model can be used to determine the interdiffusion coefficients. The present work is concerned with the diffusion-controlled growth of Cu_6Sn_5 and Cu_3Sn IMCs between Cu and Sn-based solders with high percentage

of Sn. Unless stated otherwise, the amount of Sn and Cu atoms diffused into the Cu and Sn-based solder is limited and may be ignored. Under such an assumption, the interdiffusion coefficients of the Cu and Sn-based solders can be taken as any value, e.g. the same value as the interdiffusion coefficient for the Cu_3Sn or the Cu_6Sn_5 IMCs. Furthermore, as in the existing literature [10,16,18], the interdiffusion coefficients, D_{Cu3Sn} and D_{Cu6Sn5}, for the Cu_3Sn and Cu_6Sn_5 IMCs are both assumed as material constants independent of composition. Then the thicknesses of the Cu_3Sn and Cu_6Sn_5 IMCs in a sample can be considered as a function of D_{Cu3Sn}, D_{Cu6Sn5} and time t, and can be simulated using the numerical model. The D_{Cu3Sn} and D_{Cu6Sn5} can finally be determined with the best data fittings of achieving the least sum for the square of the measured thicknesses of Cu_6Sn_5 and Cu_3Sn layers minus those simulated with the numerical model.

For all simulation cases, the initial Molar fraction gradients are assumed to be linear across the Cu_6Sn_5 and/or Cu_3Sn layers if their initial thicknesses are non-zero. In the case that the stoichiometric widths of Cu_6Sn_5 and Cu_3Sn IMCs are unknown, a small Molar fraction value, e.g. $\Delta N_i = 0.01$, is first assumed across them, and the Wagner's integrated interdiffusion coefficient can be employed and is finally calculated as:

$$D_{Int,i} = \int_{N_i^-}^{N_i^+} D_i dN_i = D_i \Delta N_i \tag{22}$$

All calculations were executed with self-written codes of the MATLAB® R2007a (The Mathworks, Inc.) on a PC computer with Intel[R] Pentium[R] Core[TM] i7 CPU 976 @ 3.20 GHz processor and 8 GB RAM. The data fittings to determine the interdiffusion coefficients were achieved using the MATLAB library function "fminsearch". The running times were in the range of about 2 h to 4 h for all the simulation cases.

3. Experimental procedure

3.1. Preparation of samples

The Sn-3.8Ag-0.7Cu/Cu samples, where the initial thicknesses of both Cu_6Sn_5 and Cu_3Sn layers were non-zero, have been prepared in the present work. The solder alloy used was commercially available near eutectic 95.5Sn-3.8Ag-0.7Cu (SAC) solder paste (Multicore). The flux in the as-received SAC solder paste had been removed through reflowing the solder paste at 260 °C in air for 5 min and then cleaning it with acetone. The Cu substrate used was commercially available 1 mm thick 99.9% pure Cu foil (Alfa Aesar). It had been cut into the coupons of 12 × 10 × 1 mm in size. The cut Cu coupons were first polished using 15, 3 and 1 μm diamond slurries, then cleaned using 15% HNO_3 solution under ultrasonic support, and finally rinsed using deionised water and acetone. Then 0.3 g of diced SAC solder was placed on each of the cleaned Cu coupons to prepare the samples with a solder layer approximately 1 mm in maximum thickness. After the solder pieces were placed on the Cu coupons, they were put into a vacuum reflow oven which was first pre-heated up at 200 °C and evacuated below 5 mbar for 3 min, and then held at the same temperature and purged with 2%$H_2$98%N_2 forming gas (450 L/min at 1.5 bar) for 5 min. The reflow was finally done at 260 °C for 10 min, also under the forming gas flow of 450 L/min at 1.5 bar, before being cooled down to room temperature within 3 min. The reflowed SAC/Cu samples were put into thermal ageing at 170 °C in air for 24, 48, 96, 191, 384, 768 and 2096 h to further observe the solid state interfacial reactions.

3.2. Identification and thickness measurement of IMCs

Metallographic cross-sections of the above SAC/Cu samples were prepared for identification and thickness measurement of IMCs. A JEOL 6400 SEM using the backscattered electron signal was employed to observe and analyse the microstructural features and take the corresponding images from the polished cross-sectional samples. The IMCs formed between the solders and the Cu substrates were identified using an Oxford Instruments ISIS energy-dispersive X-ray spectroscopy (EDXS) microanalysis system fitted on the SEM. Then the thicknesses of the IMC layers were measured using an image analysis method as detailed elsewhere [23,24]. The image analysis was done utilising the Image Processing Toolbox Version 5.0.0 of MATLAB R14SP2 (The Mathworks). For each sample, three images of 512 × 416 pixels in resolution, two of 236 × 192 or 118 × 91 μm and one of 118 × 91 or 47 × 38 μm in size, were used and the obtained data series were merged together for further statistical analysis. The resulting thicknesses were given in terms of mean and 95% confidence interval.

4. Results

4.1. Cu/Sn diffusion couples

Cu/Sn diffusion couples at 190–220 °C were investigated by Onishi and Fujibuchi [16], and they estimated the interdiffusion coefficients for the Cu_6Sn_5 and Cu_3Sn IMCs with the Heumann method. In their estimation, the change of Molar volumes of Cu and Sn atoms in forming the IMCs had been neglected during the calculation. In the present work, the thicknesses of Cu_6Sn_5 and Cu_3Sn IMCs in their Cu/Sn samples were calculated from the reported parabolic growth constants, and are employed to validate

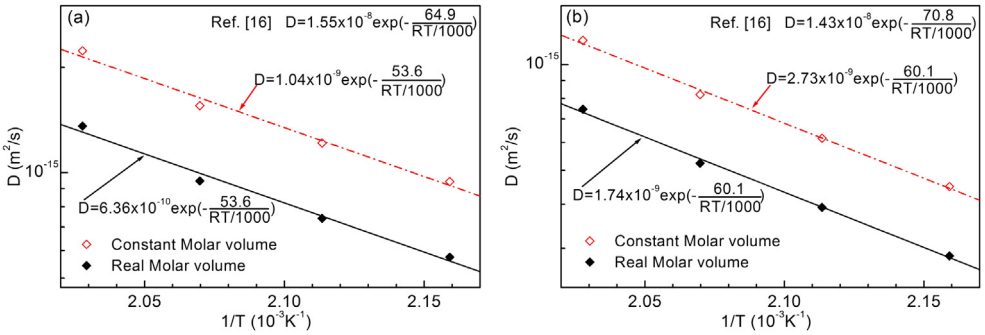

Fig. 3. Arrhenius-type plots of interdiffusion coefficients determined with the present numerical method for: (a) Cu_6Sn_5 and (b) Cu_3Sn IMCs in the Cu/Sn diffusion couples reported in Ref. [16].

the present numerical method to determine the interdiffusion coefficients. The simulated results of both constant Molar volume irrespective of phase and real Molar volume of 7.12, 8.59, 10.59 and 16.12 cm^3/mol for Cu, Cu_3Sn, Cu_6Sn_5 and Sn are given in Fig. 3. During the simulation, a fixed grid size of 0.025 μm, a small "sensible Molar fraction per Molar volume" interval, Δd, of 1.0×10^{-8} cm^3/mol, and a time step, Δt, of 3 h were used. The Molar fractions of Sn in the Cu and Sn phases were taken as 0 and 1, while the stoichiometric widths of Cu_6Sn_5 and Cu_3Sn IMCs were selected as 0.015 and 0.013 atomic fractions as reported in Ref. [16].

The interdiffusion coefficients for the Cu_6Sn_5 and Cu_3Sn IMCs determined with the present numerical method and constant Molar volume shown in Fig. 3 are almost the same as those estimated with the Heumann method and presented in Fig. 7 of Ref. [16]. However, the activation energy values of 53.6 and 60.1 kJ/mol in Fig. 3 estimated using the least square method appear to be lower than 64.8 and 70.7 kJ/mol as reported in Ref. [16]. The authors believe that this discrepancy is due to incorrect estimation by the previous researchers. As can be further seen from Fig. 3, in comparison with the interdiffusion coefficients determined with real Molar volume values for the different phases, those determined under the assumption of constant Molar volume overestimate the interdiffusion coefficients for the Cu_6Sn_5 and Cu_3Sn IMCs, by 64% and 57% respectively. Nevertheless, the activation energy values are the same as each other irrespective of using constant and real Molar volume values for the different phases.

Mei et al. [18] also estimated the interdiffusion coefficients for the Cu_6Sn_5 and Cu_3Sn IMCs formed in the above Cu/Sn diffusion couples with a combined analytical and numerical method. In their estimation, the change of Molar volumes of Cu and Sn atoms in forming the IMCs was still neglected. However, the diffusion of Cu and Sn atoms in both Cu and Sn phases was included, where the interdiffusion coefficients for the Cu and Sn phases were respectively calculated from the tracer diffusion coefficients of Sn in Cu and Cu in Sn according to the Darken-Manning treatment, and the Cu atomic factions were 0.993 and 0.00006 at the interface of Cu in contact with Cu_3Sn and the interface of Sn in contact with Cu_6Sn_5, respectively. Also, the Cu atomic fractions at the interfaces of the IMCs layers, and thereby the stoichiometric widths of the Cu_6Sn_5 and Cu_3Sn IMCs, 0.008 and 0,01, were different from those used in Ref. [16].

In the present work, the interdiffusion coefficients for the Cu_6Sn_5 and Cu_3Sn IMCs were re-calculated with the present numerical method. In this recalculation, the interface conditions of atomic fractions for the different phases and the interdiffusion coefficients for the Cu and Sn phases were the same as those used in Ref. [18]. During the numerical procedure, the relevant parameters such as Molar volume for the different phases, small "sensible Molar fraction per unit Molar volume" interval and time step used during the numerical procedure were similar to those for the results shown in Fig. 3. A uniform fixed grid size of 0.025 μm was used to discretise the central interval where the IMCs would grow, and a non-uniform fixed grid with sizes from 0.025 to 17.75 μm was used to discretise the two Cu and Sn end intervals where no phase change would occur during the simulation.

The results recalculated with present numerical method are presented in Fig. 4. The interdiffusion coefficients for the Cu_6Sn_5 and Cu_3Sn IMCs and their activation energies for constant Molar volume irrespective of phase are all in excellent agreement with those reported by Mei et al. [18]. Also, similar to the results shown in Fig. 3, in comparison with the interdiffusion coefficients determined with real Molar volume values for the different phases, those determined under the assumption of constant Molar volume overestimate the interdiffusion coefficients for the Cu_6Sn_5 and Cu_3Sn IMCs, by 66% and 63% respectively. Nevertheless, the activation energy values are the same as each other irrespective of using constant and real Molar volume values for the different phases.

Furthermore, it can be seen that the activation energy values shown in Fig. 4 are slightly different from, but almost the same as those shown in Fig. 3 for the interdiffusion coefficients of both the Cu_6Sn_5 and Cu_3Sn IMCs. Using Eq. (22) and the stoichiometric widths of Cu_6Sn_5 and Cu_3Sn IMCs used during the simulation, all the interdiffusion coefficient values of the points shown in Figs. 3 and 4 can be converted into the corresponding integrated interdiffusion coefficients. The integrated interdiffusion coefficients converted from the results shown in Fig. 4 are also slightly different, but almost the same as those converted from the results shown in Fig. 3 provided that they are the results under the same assumption of using constant or real Molar volume values for the different phases. The slight difference in the activation energy values and the converted integrated interdiffusion coefficients can be attributed to the effect of the diffusion of Cu and Sn atoms in the Cu and Sn phases which were included in the simulation cases for Fig. 4, but not in the simulation cases for Fig. 3.

4.2. Cu/Cu_6Sn_5 and Cu_3Sn/Sn diffusion couples

Paul et al. [10] investigated one Cu/Sn diffusion couple at 200 °C, six Cu/Cu_6Sn_5 diffusion couples at 225–350 °C and three Cu_3Sn/Sn diffusion couples at 150–200 °C. They estimated the integrated interdiffusion coefficients for the Cu_6Sn_5 and Cu_3Sn IMCs with Wagner's method. In their estimation, only the Molar volume values of Cu_6Sn_5 and Cu_3Sn IMCs were needed during estimation of the integrated interdiffusion coefficients for the Cu_6Sn_5 and Cu_3Sn IMCs in the Cu/Sn diffusion couple, and no Molar volume of any phase was required during estimation of the integrated interdiffusion coefficients for the Cu_6Sn_5 and Cu_3Sn IMCs in the three Cu_3Sn/Sn or six Cu/Cu_6Sn_5 diffusion couples.

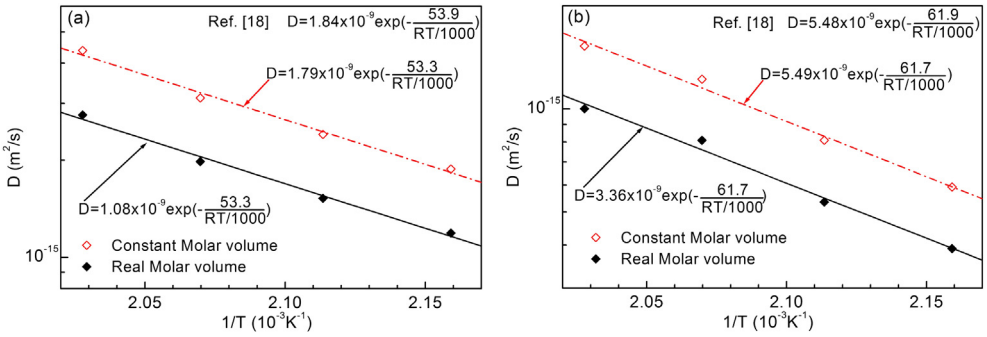

Fig. 4. Arrhenius-type plots of interdiffusion coefficients determined with the present numerical method for: (a) Cu_6Sn_5 and (b) Cu_3Sn IMCs in the Cu/Sn diffusion couples reported in Ref. [18].

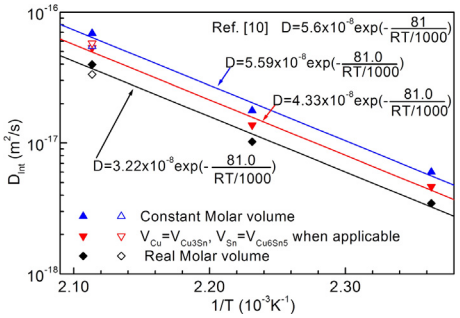

Fig. 5. Arrhenius-type plots of integrated interdiffusion coefficients determined with the present numerical method for Cu_6Sn_5 IMC formed in three Cu_3Sn/Sn diffusion couples and one Cu/Sn diffusion couple reported in Ref. [10]. The solid points are results of the three Cu_3Sn/Sn diffusion couples, and the open points are results of the Cu/Sn diffusion couple.

In the present work, the thicknesses of Cu_6Sn_5 and Cu_3Sn layers reported or calculated from the reported parabolic growth constants in Ref. [10] are employed to further validate the present numerical method to determine the integrated interdiffusion coefficients. The relevant parameters such as Molar volume for the different phases, fixed grid size, small "sensible Molar fraction per unit Molar volume" interval and time step used during the numerical procedure were similar to those for the results shown in Fig. 3. However, because the stoichiometric widths of both Cu_6Sn_5 and Cu_3Sn IMCs were unknown and are temporarily needed for the present numerical scheme, a value of 0.01 atomic fraction was randomly used for both of them. The results are presented in terms of integrated interdiffusion coefficients calculated with Eq. (22) and shown in Figs. 5 and 6. It should be pointed out that any values of the atomic fractions in the range of 0.001–0.1 chosen as the temporary stoichiometric widths of Cu_6Sn_5 and Cu_3Sn IMCs were proven to produce the same integrated interdiffusion coefficients.

The integrated interdiffusion coefficients and their activation energy values for the Cu_6Sn_5 and Cu_3Sn IMCs determined with the present numerical method and $V_{Sn} = V_{Cu6Sn5}$ and $V_{Cu} = V_{Cu3Sn}$ for the Cu/Sn diffusion couple, and constant Molar volume for the Cu/Cu_6Sn_5 and Cu_3Sn/Sn diffusion couples, are all in excellent agreement with those reported by Paul et al. [10]. With real Molar volume values for the different phases, the present results of the integrated interdiffusion coefficients for the Cu_6Sn_5 and Cu_3Sn IMCs in the Cu_3Sn/Sn and Cu/Cu_6Sn_5 diffusion couples are 42% and 24% lower than those reported by Paul et al., respectively. Nevertheless, the activation energy values are the same as each other irrespective

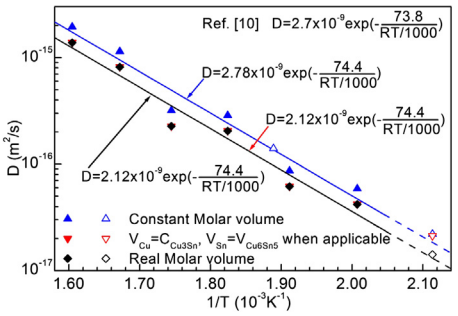

Fig. 6. Arrhenius-type plots of integrated interdiffusion coefficients determined with the present numerical method for Cu_3Sn IMC formed in six Cu/Cu_6Sn_5 diffusion couples and one Cu/Sn diffusion couple reported in Ref. [10]. The solid points are results of the six Cu/Cu_6Sn_5 diffusion couples, and the open points are results of the Cu/Sn diffusion couple.

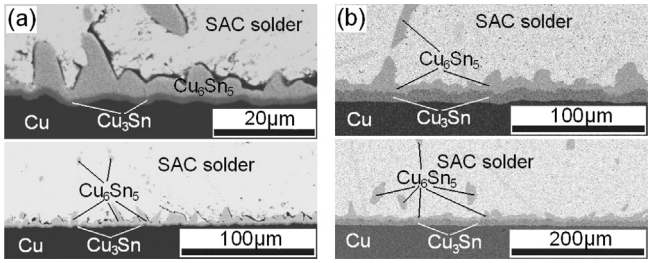

Fig. 7. SEM images taken from the polished cross sections of the SAC/Cu samples aged at 170 °C for: (a) 24 h; and (b) 2076 h.

of using constant and real Molar volume values for the different phases.

4.3. SAC/Cu samples

EDXS analysis revealed that two distinct layers of IMCs can be observed in all SAC/Cu samples. After the SAC/Cu samples reflowed at 260 °C for 10 min were put into ageing at 170 °C, the interface between the Cu_6Sn_5 layer and the solder in the samples gradually became planar (Fig. 7). However, a few protruding Cu_6Sn_5 grains were still on the Cu_6Sn_5 layer in the SAC/Cu sample even after an ageing time of 2076 h (Fig. 7b). The measured thicknesses of the Cu_6Sn_5 and Cu_3Sn layers in the aged SAC/Cu samples are presented in Fig. 8, together with the thicknesses and integrated interdiffusion coefficients calculated and extracted using the current numerical method. Note that here dispersive IMC grains within the bulk of the solder are excluded in the estimation of the thickness, and the error bars stand for the 95% confidence intervals of the mean thicknesses. During the numerical procedure, the thicknesses of the Cu_6Sn_5 and Cu_3Sn layers in the SAC/Cu sample reflowed at 260 °C for 10 min were taken as the initial conditions. In addition, a smaller "sensible Molar fraction per Molar volume" interval of 1.0×10^{-9} cm^3/mol and a time step of 17.3 h was used, while the other relevant parameters for the numerical procedure were the same as those for the results shown in Figs. 5 and 6.

The thicknesses calculated using the present numerical model agree with the measured mean thicknesses satisfactorily. For ageing times between 24 and 191 h, both the measured and calculated thicknesses of the Cu_6Sn_5 layer appear to be thinner than that for the as-flowed sample. For ageing times of 384–2096 h, the thicknesses of the Cu_6Sn_5 layer increase with increasing ageing time. By contrast, both the measured and calculated thicknesses of the Cu_3Sn layers increase with ageing time from the start. The extracted $D_{int,Cu3Sn}$ and $D_{int,Cu6Sn5}$ for the best data fitting are 8.25×10^{-19} m^2/s and 9.97×10^{-19} m^2/s, respectively.

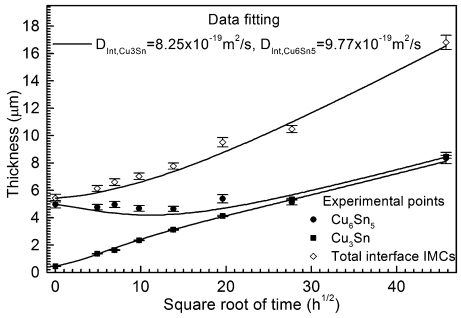

Fig. 8. Plots of thickness versus square root of time for IMCs formed at interfaces in the SAC/Cu samples during thermal ageing at 170 °C.

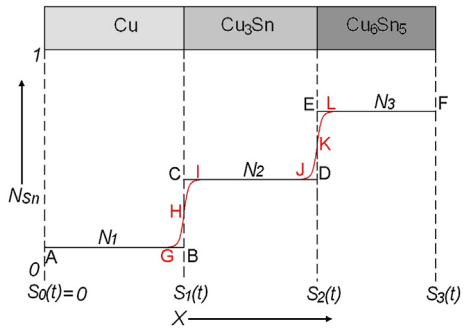

Fig. 9. Schematic illustration of the realistic profile ABCDEF and extended continuous and differentiable profile AGHIJKLF for Molar fraction N_{Sn} across a Cu/Cu_6Sn_5 diffusion couple at the instant time of *t*.

5. Discussion

5.1. Validation of the present numerical method

The present numerical approach develops an iteration method to solve an inverse problem for calculating the interdiffusion coefficients from the measured thicknesses of Cu_6Sn_5 and Cu_3Sn IMC layers. For any of the above simulation cases, the calculated interdiffusion coefficients were always converged towards the same values irrespective of initially guessed values. Therefore, from a viewpoint of mathematics, the interdiffusion coefficients or integrated interdiffusion coefficients determined using the present numerical method are unique.

As verified by Figs. 3 and 4, if ignoring the change of Molar volumes of Cu and Sn atoms in forming the IMCs, the presently developed numerical method can be used to extract the interdiffusion coefficients for the Cu_6Sn_5 and Cu_3Sn IMCS yielding results almost the same as those of the Heumann method and a combined analytical and numerical method reported in Ref. [16,18]. This demonstrates that there is no fundamental numerical error when the presently developed numerical method is used to determine the interdiffusion coefficients or integrated interdiffusion coefficients.

As shown in Figs. 5 and 6, the presently developed numerical method requires additional assumptions of $V_{Cu} = V_{Cu3Sn}$ and $V_{Sn} = V_{Cu6Sn5}$ for the Cu/Sn diffusion couple, and constant Molar volume irrespective of phase and composition for the Cu_3Sn/Sn or Cu/Cu_6Sn_5 diffusion couples to extract the integrated interdiffusion coefficients for the Cu_6Sn_5 and Cu_3Sn IMCS the same as those of the Wagner's method [10]. However, such additional assumptions are reasonable and can be explained as follows. First, it is hard to understand that the actual integrated interdiffusion coefficients for the Cu_6Sn_5 and Cu_3Sn IMCS in the Cu_3Sn/Sn and Cu/Cu_6Sn_5 diffusion couples are independent of the Molar volume values of the different phases. Furthermore, a systematic error can be found in the use of Wager's equations to calculate the integrated interdiffusion coefficients for the Cu_6Sn_5 and Cu_3Sn IMCS as detailed below.

According to the well known calculus theorem, any differentiable function must be continuous at every point in its domain, in Wagner's deduction, J_1 and J_2 in the Eqs. (7)–(11) must be continuous between $\lambda = -\infty$ and $\lambda = \lambda^*$, and between $\lambda = \lambda^*$ and $\lambda = \infty$ in order to calculate their derivatives for deriving Eq. (12) in Ref. [17]. In order to apply Eq. (12) in Ref. [17], Cu and Sn atomic fractions at the interfaces of the different phases in the Cu/Sn, Cu_3Sn/Sn and Cu/Cu_6Sn_5 diffusion couples must modified and approximated as continuous and differentiable functions of position coordinate of *x*. This can be illustrated with the Cu/Cu_6Sn_5 diffusion couple as one example as shown in Fig. 9. Here one continuous and differentiable curve GHI is used to approximate the two separate segments GB and CI, and another continuous and differentiable curve JKL is used to approximate the two separate segments JD and EL for describing the distribution of Sn atomic fraction with respect to position coordinate of *x*. Following Eq. (12) in Ref. [17], we can derive:

$$\begin{aligned} D_{Int,IJ} = {} & \frac{(N_2-N_1)(N_3-N_2)}{(N_3-N_1)}\frac{\Delta x_{IJ}^2}{2t} \\ & + \frac{(N_3-N_2)}{(N_3-N_1)}\left[\int_{x_G}^{x_H}\frac{V_{Cu3Sn}}{V_{Cu}}(N_{Sn}-N_1)dx \right. \\ & \left. + \int_{x_H}^{x_I}(N_{Sn}-N_1)dx\right]\frac{\Delta x_{IJ}}{2t} + \frac{(N_2-N_1)}{(N_3-N_1)}\left[\int_{x_J}^{x_K}(N_3-N_{Sn})dx \right. \\ & \left. + \int_{x_K}^{x_L}\frac{V_{Cu3Sn}}{V_{Cu6Sn5}}(N_3-N_{Sn})dx\right]\frac{\Delta x_{IJ}}{2t} \end{aligned} \tag{23}$$

Then the integrated interdiffusion coefficient for the Cu_3Sn IMC with CD being as the distribution of Sn atomic fraction can be calculated by linearly extrapolating the above Eq. (23) for the Cu_3Sn IMC with IJ being as the distribution of Sn atomic fraction and expressed as:

$$D_{Int,Cu3Sn} = D_{Int,IJ}\times\frac{\Delta x_{CD}}{\Delta x_{IJ}} \tag{24}$$

In this way, the equality of diffusion fluxes both within the Cu_3Sn IMC and at the Cu/Cu_3Sn and Cu_3Sn/Cu_6Sn_5 interfaces can be guaranteed. Furthermore, without affecting the validity, we may take GB = CI = JD = EL = δ*x*, GH and IH are symmetrical relative to centre H, and JK and LK are symmetrical relative to centre K. Then only under the assumption of $V_{Cu} = V_{Cu3Sn} = V_{Cu6Sn5}$, from Eqs. (23) and (24), we can obtain the following Eq. (25) that is the same as Eq. (21) in Ref. [17] for calculating the integrated interdiffusion coefficient of the Cu_3Sn IMC.

$$\begin{aligned} D_{Int,Cu3Sn} &= \frac{(N_2-N_1)(N_3-N_2)}{2t(N_3-N_1)}\left[(\Delta x_{IJ}+2\delta x)\Delta x_{IJ}+2\delta x(\Delta x_{IJ}+2\delta x)\right] \\ &= \frac{(N_2-N_1)(N_3-N_2)}{(N_3-N_1)}\frac{\Delta x_{Cu3Sn}^2}{2t} \end{aligned} \tag{25}$$

Otherwise, there will be inequality of diffusion fluxes at interfaces of the different phases if Eq. (25) is used to calculate the integrated interdiffusion coefficient of the Cu_3Sn IMC. Similarly, it can be elucidated that only under the assumption of $V_{Cu} = V_{Cu3Sn}$ and $V_{Sn} = V_{Cu6Sn5}$ or constant Molar volume for the different phases, Eqs. (20) and (21) in Ref. [17] can be used to calculate the integrated interdiffusion coefficients for the Cu_6Sn_5 and Cu_3Sn IMCS in the Cu/Sn and Cu_3Sn/Sn diffusion couples. With real Molar volumes for the different phases, Eqs. (20) and (21) are not consistent with Eq. (12) in Ref. [17]. There will be inequality of diffusion fluxes at the interfaces and hence a systematic error when Eqs. (20) and (21) in Ref. [17] are used to calculate the integrated interdiffusion coefficients.

Using the real Molar volume values for the different phases, the present numerical method produces lower estimations of the interdiffusion coefficients or integrated interdiffusion coefficients for the Cu_6Sn_5 and Cu_3Sn IMCS than the Heumann method, the Wagner's method and a combined analytical and numerical method in the existing literature [10,16,18]. However, if all the interdiffusion coefficients or integrated interdiffusion coefficients were estimated using the same method, they would have no

appreciable effect on deriving the corresponding activation energy values.

Despite the fact that the values of $D_{Int,Cu3Sn}$ and $D_{Int,Cu6Sn5}$ overestimated under the assumption of $V_{Cu} = V_{Cu3Sn}$ and $V_{Sn} = V_{Cu6Sn5}$ can still be used to predict the thicknesses of Cu_6Sn_5 and Cu_3Sn layers, all the interfaces of the different phases simulated under such an assumption are moved towards the Cu side, as can be seen from Fig. 10. This means that the consumption of Cu would be overestimated and the consumption of Sn would be underestimated, when compared to those simulated with the correct values of $D_{Int,Cu3Sn}$ and $D_{Int,Cu6Sn5}$ and real Molar volume values of the different phases. The overestimations in the interdiffusion coefficients or integrated interdiffusion coefficients can be corrected, but the correction constants depend on the diffusion couples as shown in Figs. 3–6. Such a result demonstrates that without correction, the interdiffusion coefficients or integrated interdiffusion coefficients estimated using the Heumann method and Wagner's method from the Cu/Cu_6Sn_5 and Cu_3Sn/Sn diffusion couples cannot directly be applied to the Cu/Sn diffusion couples.

Ronka et al. [4] developed a combined thermodynamic and diffusion-kinetic model, and applied it to predict the growth of Cu_6Sn_5 and Cu_3Sn IMCS in binary solid/solid Cu/Sn systems and ternary solid/solid and solid/liquid Cu/Sn–Bi systems. In the ternary systems, the integrated interdiffusion coefficients are not material constants anymore, so they employed tracer diffusion coefficients as materials constants to calculate and update the integrated interdiffusion coefficients depending on the composition of the Sn–Bi solder. Such an approach can be incorporated into the present numerical model without any difficulty. In comparison with Ronka et al.'s model, the present numerical model can take account of the effect of the Molar volume of Cu on the kinetics, and more easily be extended to multi-component, multi-phase systems and high-dimensional problems, without the need of tracing the mass balance of atoms diffused across the moving interfaces of the different phases. Also, it is convenient to incorporate other physical phenomena, e.g. convection caused by fluid flow into the present numerical model when necessary. This is because the present numerical method has been developed by adopting the fixed-grid source-based method originally developed to simulate the temperature fields for melting-solidification phase change processes [19–21]. Similar to the treatment in analysis of heat transfer, it is straightforward to extend the present model to multi-phase systems and high-dimensional problems, as well as incorporate other physical phenomena.

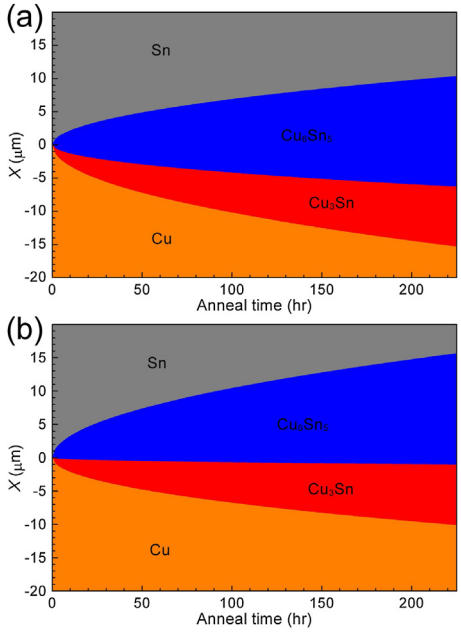

Fig. 10. The evolution of the different interfaces in the Cu/Sn diffusion couple at 200 °C that was reported in Ref. [10], simulated using the present numerical model with: (a) $D_{Int,Cu6Sn5} = 1.94 \times 10^{-17}$ m^2/s, $D_{Int,Cu6Sn5} = 5.64 \times 10^{-17}$ m^2/s, $V_{Cu} = V_{Cu3Sn} = 8.59$ cm^3/mol and $V_{Sn} = V_{Cu6Sn5} = 10.59$ cm^3/mol; and (b) $D_{Int,Cu6Sn5} = 1.41 \times 10^{-17}$ m^2/s, $D_{Int,Cu6Sn5} = 3.35 \times 10^{-17}$ m^2/s, $V_{Cu} = 7.12$ cm^3/mol, $V_{Cu3Sn} = 8.59$ cm^3/mol, $V_{Sn} = 10.59$ cm^3/mol and $V_{Cu6Sn5} = 16.12$ cm^3/mol.

5.2. Interdiffusion coefficients of the current SAC/Cu samples

The present work is concerned with the diffusion-controlled growth of the Cu_6Sn_5 and Cu_3Sn IMCs only. It is widely accepted to use diffusion-controlled growth to describe the growth kinetics of the Cu_6Sn_5 and Cu_3Sn layers in solid/solid Cu/Sn-based solder interfacial reactions. Indeed, as can be seen from Fig. 8, the data fittings of the calculated thicknesses of Cu_6Sn_5 and Cu_3Sn layers to the measured results for the SAC/Cu samples aged at 170 °C are satisfactory. However, the values of 8.25×10^{-19} m^2/s and 9.97×10^{-19} m^2/s for $D_{int,Cu3Sn}$ and $D_{int,Cu6Sn5}$ in Fig. 8, extracted from the present SAC/Cu samples aged at 170 °C, are both lower than all those interpolated or extrapolated and calculated from the results of the Cu/Sn, Cu/Cu_6Sn_5 and Cu_3Sn/Sn diffusion couples in Figs. 3–6.

As can be seen in Fig. 7, there were some isolated Cu_6Sn_5 grains existing in the SAC/Cu samples. During the prolonged isothermal ageing process, they might form a mass flow due to coalescence to cause an additional growth superimposing to the diffusion-controlled growth of the Cu_6Sn_5 layer. This would actually lead to an increase in the extracted integrated interdiffusion coefficient $D_{Int,Cu6Sn5}$.

In a previous work [25], the growth rate of Cu_3Sn in the Cu/Sn–Bi samples was found to depend on the sizes and crystalline orientation of the original Cu crystals. In another work [9], it was reported that the activation energy for parabolic growth constant of Cu_6Sn_5 IMC in Cu/Sn-3.5Ag samples during isothermal ageing depended on the method of sample preparation. The activation energy for the samples prepared using the dipping method was found to be lower than that for the samples prepared using the reflow method. Therefore, the lower $D_{Int,Cu3Sn}$ and $D_{Int,Cu6Sn5}$ in Fig. 8 are more probably related to the Cu substrate and/or the reflow process under forming gas used to prepare the as-reflowed samples.

Other values for interdiffusion coefficients or integrated interdiffusion coefficients for the Cu_6Sn_5 and Cu_3Sn IMCs formed in other Cu_3Sn/Sn and Cu/Cu_6Sn_5 diffusion couples have been reported in Refs. [16] and reviewed in Ref. [3]. However, it is difficult to compare the values of $D_{Int,Cu3Sn}$ and $D_{Int,Cu6Sn5}$ extracted from the present SAC/Cu samples with them because of the following two reasons. On the one hand, the reported interdiffusion coefficient or integrated interdiffusion coefficient data need to be corrected to account for the real Molar volume values of the different phases in the samples. On the other hand and more seriously, there is disagreement between the data presented in the existing literature. For example, the thicknesses of IMCs recalculated by the present authors with the parabolic constants listed in Table 2 appear to be inconsistent with the results plotted in Fig. 8 in Ref. [16].

6. Conclusions

A numerical method has been developed to simulate the thicknesses and extract the interdiffusion coefficients or integrated interdiffusion coefficients for diffusion-controlled growth of Cu_6Sn_5 and Cu_3Sn IMCs and this method may be applied to other systems

with many layers of IMCs. Based on results obtained, the following conclusions are drawn:

1). Under certain assumptions for the Molar volume values of the different phases, the present numerical method can produce values for the interdiffusion coefficients or integrated interdiffusion coefficients almost the same as those estimated with the Heumann method, the Wagner's method and a combined analytical and numerical method for the Cu_6Sn_5 and Cu_3Sn IMCs formed in the Cu/Sn, Cu/Cu_6Sn_5 and Cu_3Sn/Sn diffusion couples.
2). Using real Molar volume values of the different phases, the present numerical method produce values for the interdiffusion coefficients or integrated interdiffusion coefficients clearly lower than those estimated with the Heumann method, the Wagner's method and a combined analytical and numerical method. The extent of discrepancy in the interdiffusion coefficients or integrated interdiffusion coefficients depends on the specific diffusion couples.
3). The present numerical method should be more accurate than the Heumann method and the Wagner's method in their existing forms. This is because the change of Molar volumes of Cu and Sn atoms in forming the IMCs was neglected in the Heumann method, and a systematic error can be identified in the use of Wagner's equation to calculate the integrated interdiffusion coefficients for the Cu_6Sn_5 and Cu_3Sn IMCs. Furthermore, the interdiffusion coefficients or integrated interdiffusion coefficients estimated with the Heumann method and the Wagner's method can simply be calibrated with the results determined with present numerical method.
4). The present numerical method can be applied to diffusion couples with arbitrary initial thicknesses of the different phases, and easily extended to multi-component, multi-phase systems and high-dimensional problems, without the need of tracing the mass balance of atoms diffused across the moving interfaces of the different phases.
5). The growth kinetics of the Cu_6Sn_5 and Cu_3Sn layers in the SnAgCu/Cu samples during the solid/solid interface reaction can be fitted well to the present numerical model. However, the extracted integrated interdiffusion coefficients for the Cu_6Sn_5 and Cu_3Sn IMCs appeared to be lower than those interpolated or extrapolated and calculated from the results of the Cu/Sn, Cu/Cu_6Sn_5 and Cu_3Sn/Sn diffusion couples. This may be ascribed to the Cu substrate and/or the reflow process under forming gas used to prepare the as-reflowed samples.

Acknowledgements

This research was supported by the UK Engineering and Physical Science Research Council as part of the Innovative Electronic Manufacturing Research Centre (IeMRC) [grant number EP/H03014X/1].

References

[1] Zeng K, Tu KN. Six cases of reliability study of Pb-free solder joints in electronic packaging technology. Mater Sci Eng 2002;R38(2):55–105.
[2] Wu CML, Yu DQ, Law CMT, Wang L. Properties of lead-free solder alloys with rare earth element additions. Mater Sci Eng 2004;R44(1):1–44.
[3] Laurila T, Vuorinen V, Kivilahti JK. Interfacial reactions between lead-free solders and common base materials. Mater Sci Eng 2005;R49(1–2):1–60.
[4] Ronka KJ, Van Loo FJJ, Kivilahti JK. A diffusion-kinetic model for predicting solder/conductor interactions in high density interconnections. Metall Mater Trans 1998;28A(12):2951–6.
[5] Kim HK, Tu KN. Kinetic analysis of the soldering reaction between eutectic SnPb alloy and Cu accompanied by ripening. Phys Rev 1996;B53(23):16027–34.
[6] Schaefer M, Fournelle RA, Liang J. Theory for intermetallic phase growth between Cu and liquid Sn-Pb solder based on grain boundary diffusion control. J Electron Mater 1998;27(11):1167–76.
[7] Gusak AM, Tu KN. Kinetic theory of flux-driven ripening. Phys Rev 2002;B66(11):115403/1–115403/14.
[8] Flanders DR, Jacobs EG, Pinizzotto RF. Activation energy of intermetallic growth of Sn-Ag eutectic solder on copper substrates. J Electron Mater 1997;26(7):883–7.
[9] Yu DQ, Wu CML, Law CMT, Wang L, Lai JKL. Intermetallic compounds growth between Sn-3.5Ag lead-free solder and Cu substrate by dipping method. J Alloys Comp 2005;392(1–2):192–9.
[10] Paul A, Ghosh C, Boettinger WJ. Diffusion parameters and growth mechanism of phases in the Cu-Sn system. Metall Mater Trans 2011;42A(4):952–63.
[11] Prakash KH, Sritharan T. Interface reaction between copper and molten tin-lead solders. Acta Mater 2001;49(13):2481–9.
[12] Chuang CM, Lin KL. Effect of microelements addition on the interfacial reaction between Sn-Ag-Cu solders and the Cu substrate. J Electron Mater 2003;32(12):1426–31.
[13] Takaku Y, Liu XJ, Ohnuma I, Kainuma R, Ishida K. Interfacial reaction and morphology between molten Sn base solders and Cu substrate. Mater Ttrans 2004;45(3):646–51.
[14] Liang J, Dariavach N, Callahan P, Shangguan D. Metallurgy and kinetics of liquid-solid interfacial reaction during lead-free soldering. Mater Ttrans 2006;47(2):317–25.
[15] Ghosh G. Coarsening kinetics of Ni_3Sn_4 scallops during interfacial reaction between liquid eutectic solders and Cu/Ni/Pd metallization. J Appl Phys 2000;88(11):6887–96.
[16] Onishi M, Fujibuchi H. Reaction-diffusion in the Cu-Sn system. Trans Jpn Inst Met 1975;16:539–47.
[17] Wagner C. The evaluation of data obtained with diffusion couples of binary single-phase and multiphase systems. Acta Metall 1969;17:99-1–99-7.
[18] Mei Z, Sunwoo A, Morris JW. Analysis of low-temperature intermetallic growth in copper-tin diffusion couples. Metall Mater Trans 1992;23A:857–64.
[19] Li JF, Agyakwa PA, Johnson CM. A fixed-grid numerical modelling of transient liquid phase bonding and other diffusion controlled phase changes. J Mater Sci 2010;45(9):2340–50.
[20] Voller VR, Prakash C. A fixed grid numerical modelling methodology for convection-diffusion mushy region phase-change problems. Inter J Heat Mass Trans 1987;30(8):1709–19.
[21] Kumar A, Dutta P. Numerical studies on columnar-to-equiaxed transition in directional solidification of binary alloys. J Mater Sci 2009;44(15):3952–61.
[22] Patankar SV. Numerical heat transfer and fluid flow, hemisphere. Washington, DC 198041.
[23] Montavon G, Coddet C, Berndt CC, Leigh SH. Microstructural index to quantify thermal spray deposit microstructures using image analysis. J Therm Spray Technol 1998;7(2):229–41.
[24] Li JF, Mannan SH, Clode MP, Whalley DC, Hutt DA. Interfacial reactions between molten Sn-Bi-X solders and Cu substrates for liquid solder interconnects. Acta Mater 2006;54(11):2907–22.
[25] Shang PJ, Liu ZQ, Pang XY, Li DX, Shang JK. Growth mechanisms of Cu_3Sn on polycrystalline and single crystalline Cu substrates. Acta Mater 2009;57(16):4697–706.